Self-powered Nanowire Devices

Sheng Xu#, Yong Qin#, Chen Xu#, Yaguang Wei, Rusen Yang, Zhong Lin Wang

Authors with equal contribution

"Self-powered" system

A totally self-powered nanosystem should include the nanodevices, power harvesting unit, electrical measurement system, data processing logic system, and possibly wireless communication unit (RF technology). By "self-powered" in our manuscript, we mean that the NG can power a nanodevice that is a separated unit from the NG, in responding to the change in its environment.

The contact type between Au and ZnO

The Au film on which the ZnO NWs were grown has a theoretical work function of 5.1 eV that is higher than the electron affinity of ZnO (4.5 eV). Thus, a Schottky barrier was supposed to form at the interface. But in reality, during the wet chemical growth of the ZnO NWs, the interface between the Au film and the ZnO NWs was not fresh owing to adsorption of organic contaminates and inclusion of inorganic impurities from the reaction solution. Consequently, the density of the interface states between the two was expected to be much higher than a clean interface. The formation of Ohmic contact was possible, and it has to be measured experimentally (see Fig. S1).

Difference in comparison to MEMS based energy harvesting technologies

Our approaches are substantially different from the traditional MEMS based power harvesting not only in the size of the unit, but also in the working principle and special applications. The traditional MEMS approach uses piezoelectric cantilever resonance to harvest energy that has a specific higher frequency, which is usually much higher than the frequencies in a biological system such as walking and heart beating. As for the frequency such as in wind blowing, air flow, and human activities, the cantilever based approach may not be an effective approach. Moreover, in reality, the distribution in frequency and magnitude in our living environment vary as a function of time. It is important to invent a technology that can be adopted for a range of frequencies. As for our approach, as long as there is a dynamic mechanical straining even at very low frequency such as a few Hz, we can use it to harvest energy. The technological road map

for scale up of our approach is also distinctly different from the traditional MEMS approach. Our nanogenerators can be integrated in underneath any surface, in carpet, in shoe pads, in floor, in tire, in biological system either in-vivo or in-vitro and many more.

The key to use the nanowires is that a tiny physical motion even in very small scale can be used for energy harvesting because a force in nano Newton scale can trigger a nanowire. While in MEMS, the triggering force has to be substantially large, which may prevent its application if the triggering force is small.
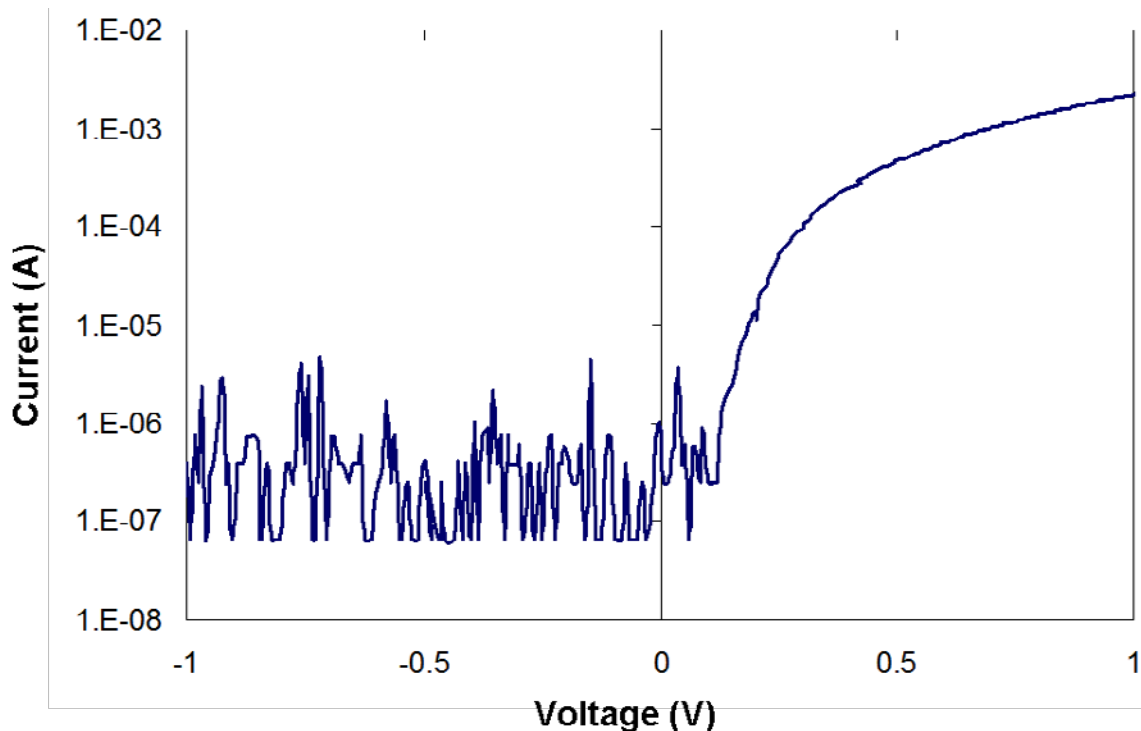

Figure S1 | A typical I-V curve of a working VING, which shows a rectification ratio of about 1000 at a biased voltage of ± 0.4 V.
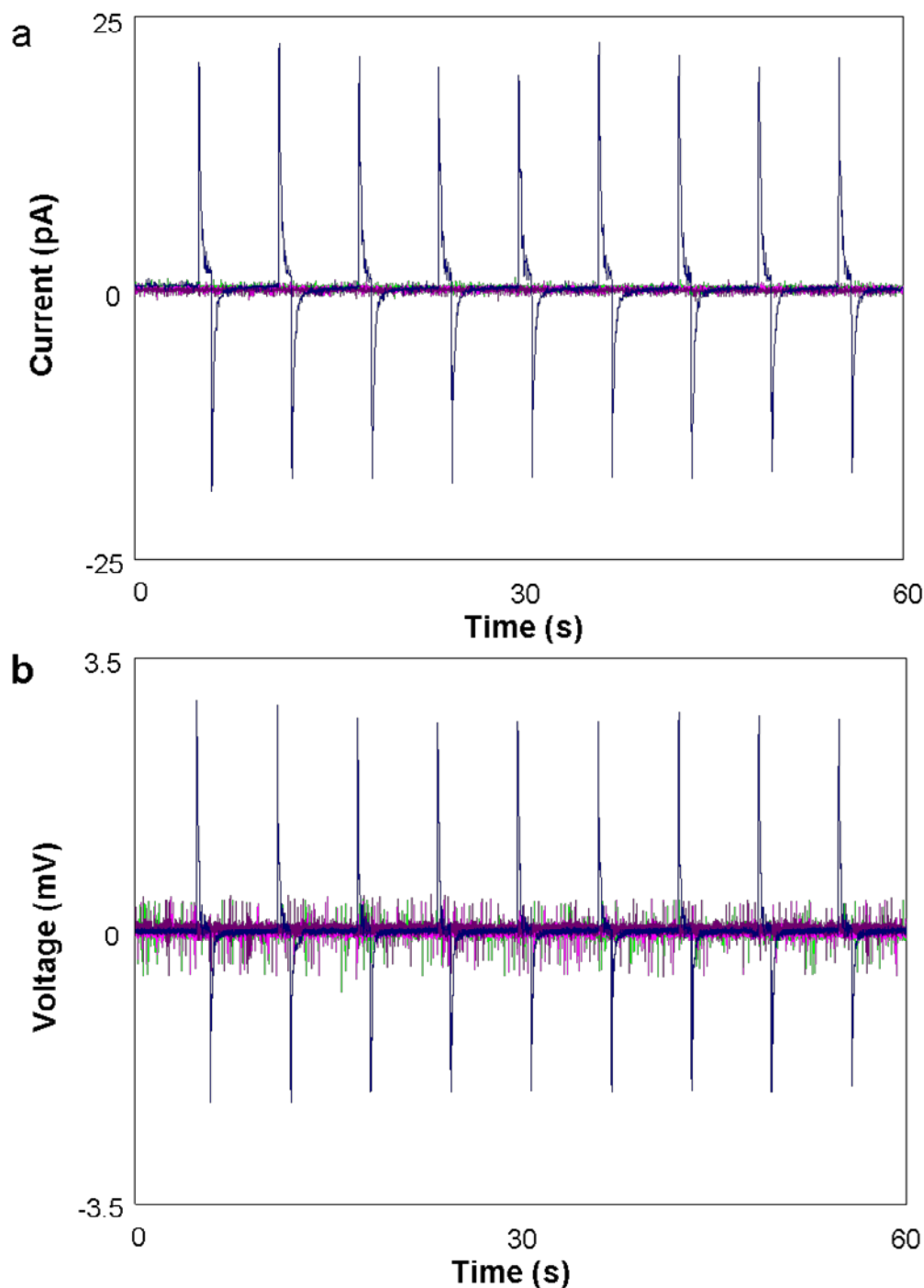
Figure S2 | Outputs (a) current and (b) voltage from a normal good working VING with Schottky transport characteristic (cyan line) and an VING with linear I–V transport characteristic (pink line), a purposely designed VING with tips of the NW fully covered by PMMA (green line), and a normal good working VING that is subjected to the mechanical action but without being physically knocked-on by the mechanical stimulator (purple line). This diagram shows that only the VING that has a Schottky contact (cyan line) produces output voltage once it is physically directly impacted.
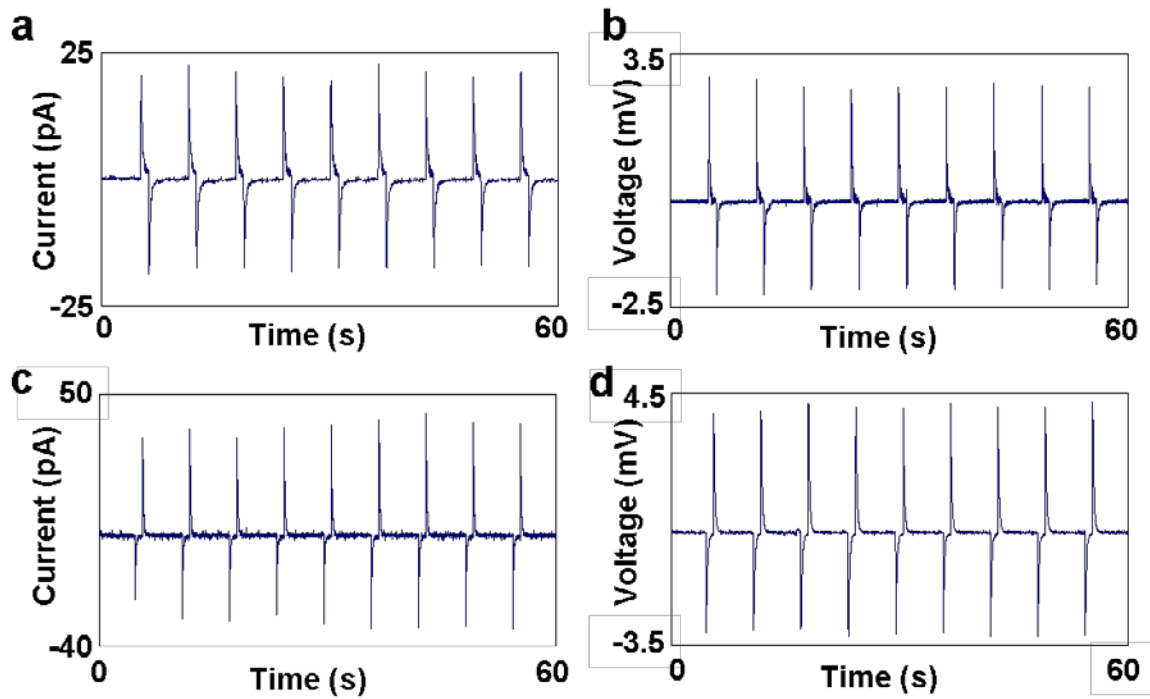
Figure S3 | Connection polarity reversion test for output current and voltage signals, respectively. The pressing force was held on the VING for 1 s before released off. Then 5 s after that, the force was re-applied onto the VING again. The reversion in output signal is apparent, just as expected.
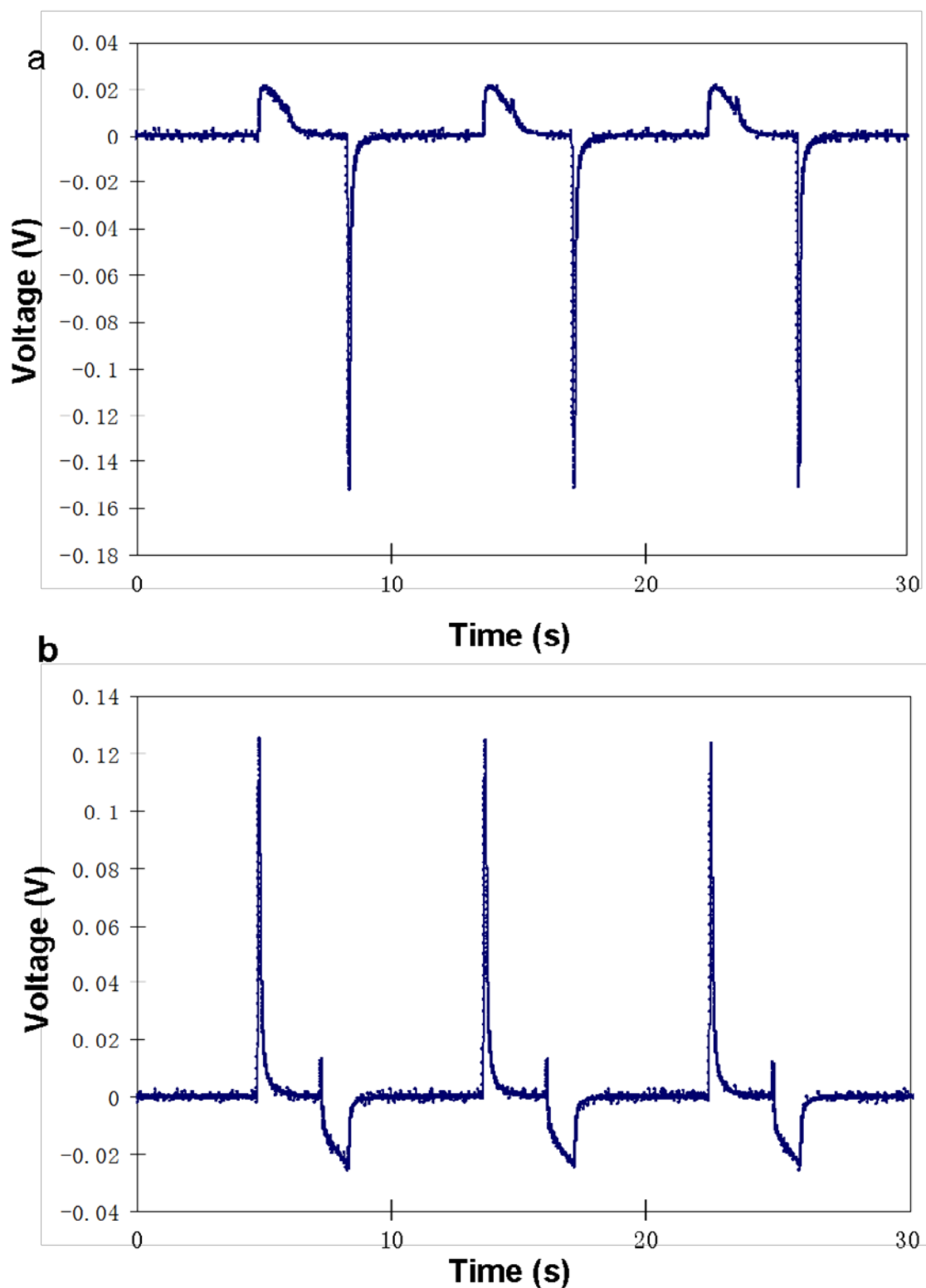
Figure S4 | Electric output voltage when an VING was subject to (a) a slow pressing and fast releasing, and (b) fast pressing and slow releasing, showing the dependence of the output voltage on the straining rate.
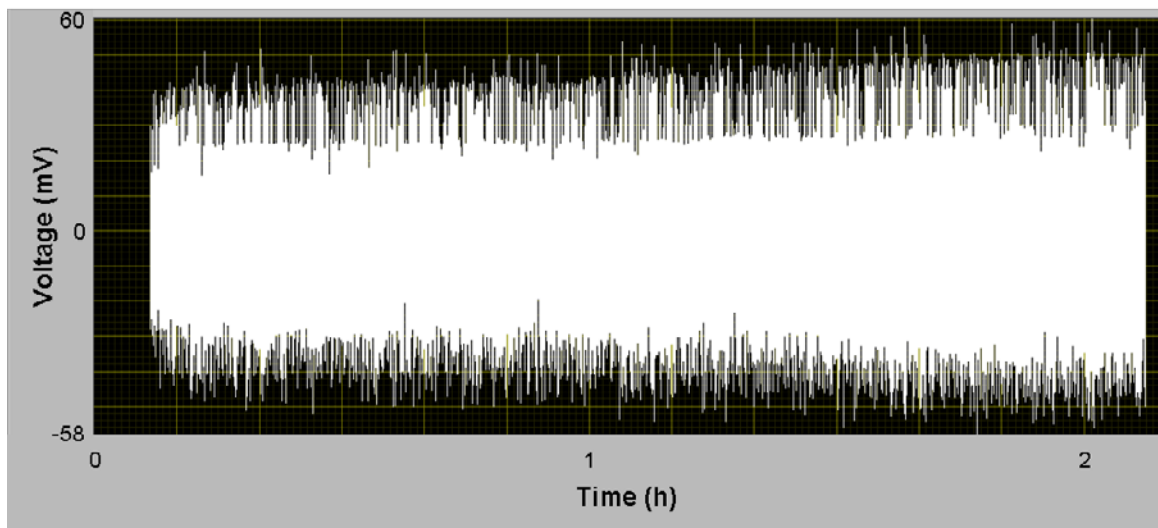
Figure S5 | Stability and robustness test of a VING. In two hours at an impacting frequency of 0.16 Hz of pressing and releasing of the VING (total 1200 cycles), the output voltage remained practically unchanged.
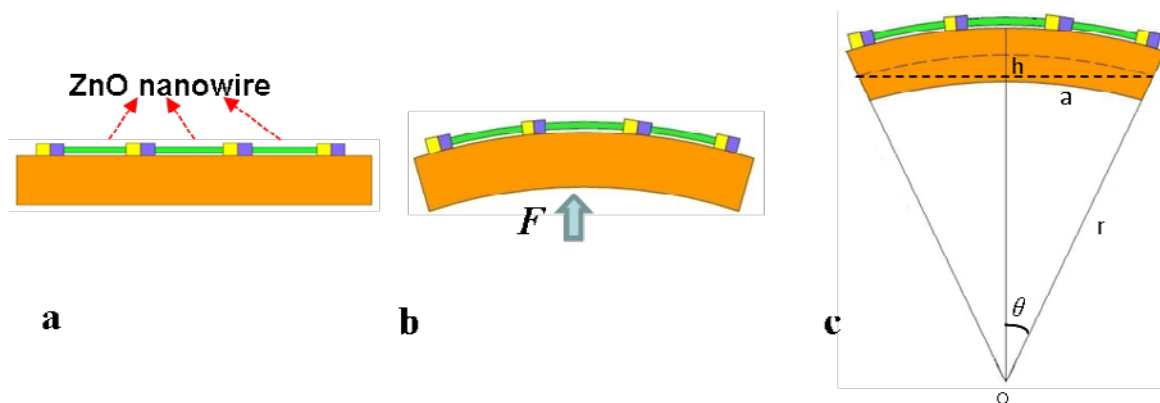
Figure S6 | Schematics showing the LING structure and the application of external force for creating tensile strain in the nanowires.

By bending the substrate into an arc shape, with a dimension as illustrated, the strain created at the outer surface is:

$$\frac{hD}{a^2 \quad h^2}$$

Where h is the height of the arc, e.g. the normal displacement of the substrate as a result of the external force impact; a is the half width of the arc; and D is the thickness of the substrate.

The straining rate at which the strain is created is:

$$v/h$$

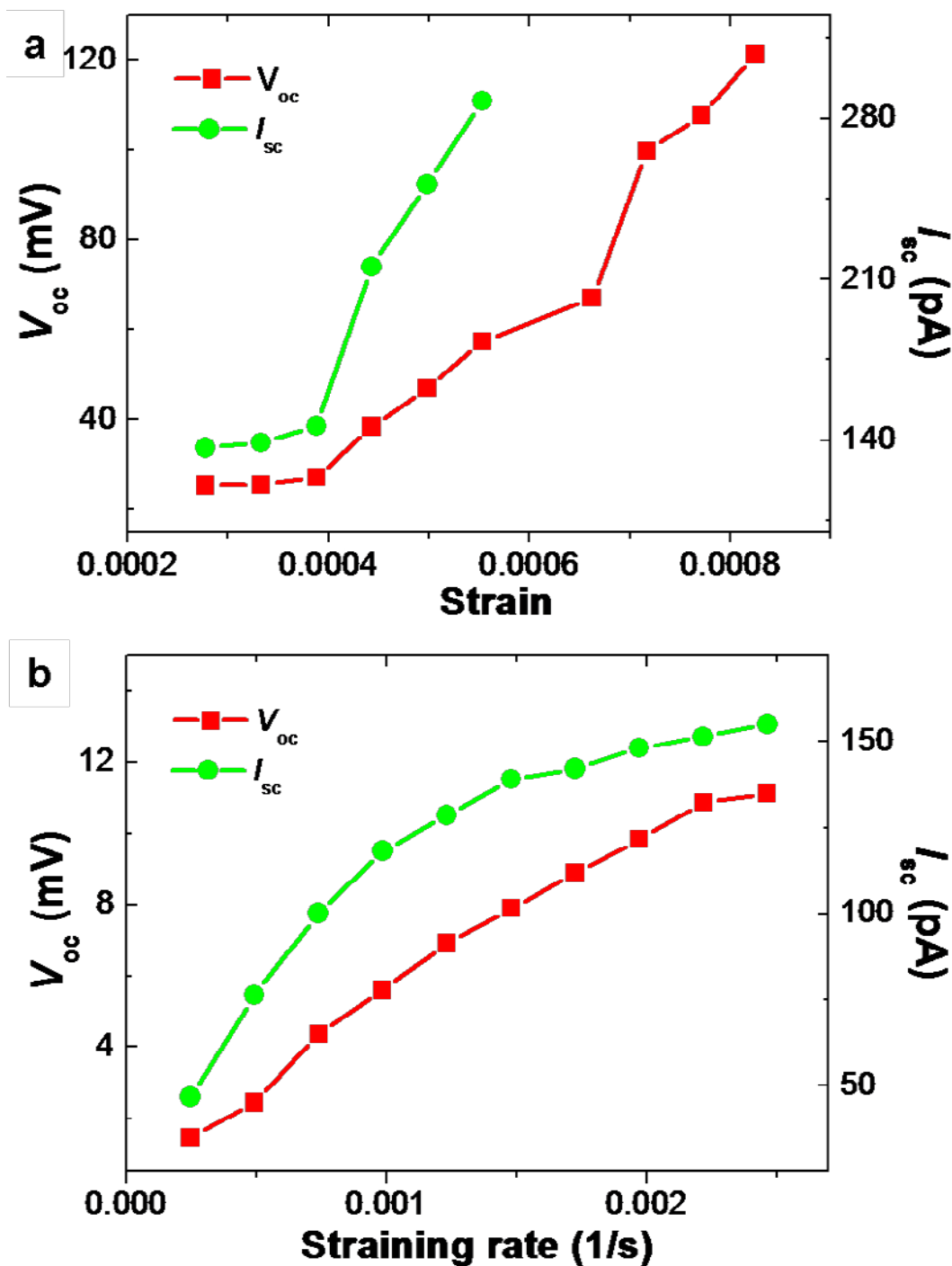Where v is the speed at which the external force impacts the substrate.

Figure S7 | (a) Open-circuit output voltage and short-circuit output current of a LING as a function of the tensile strain created in the NWs. (b) Open-circuit output voltage and short-circuit output current of a LING made of 100 rows of NWs, as a function of the straining rate at which the LING is deformed by the mechanical stimulator. The maximum strain remains 0.025%.
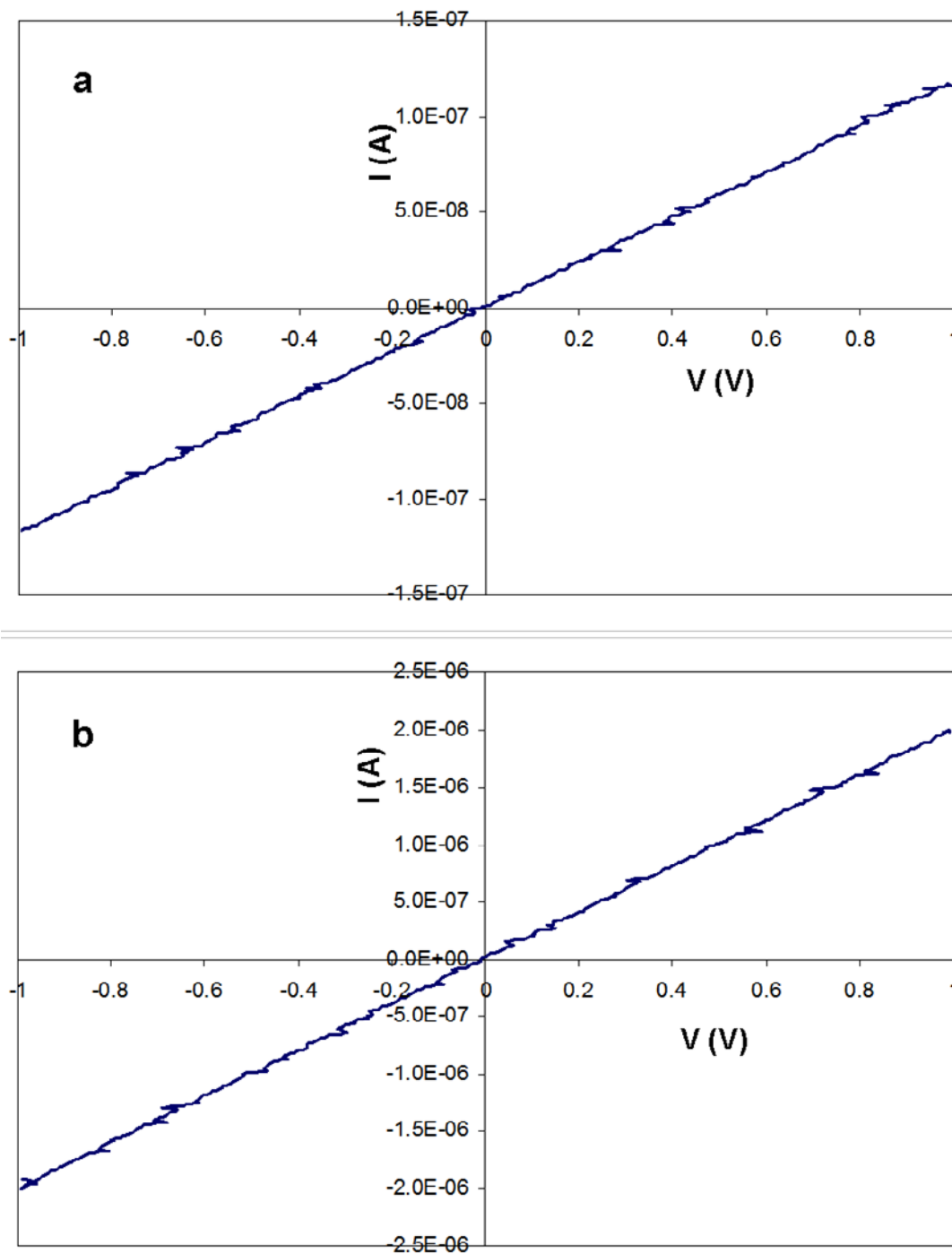
Figure S8 | I-V curve of a ZnO single NW base UV sensor (a) before and (b) after being illuminated with UV light, showing a big change in resistance.
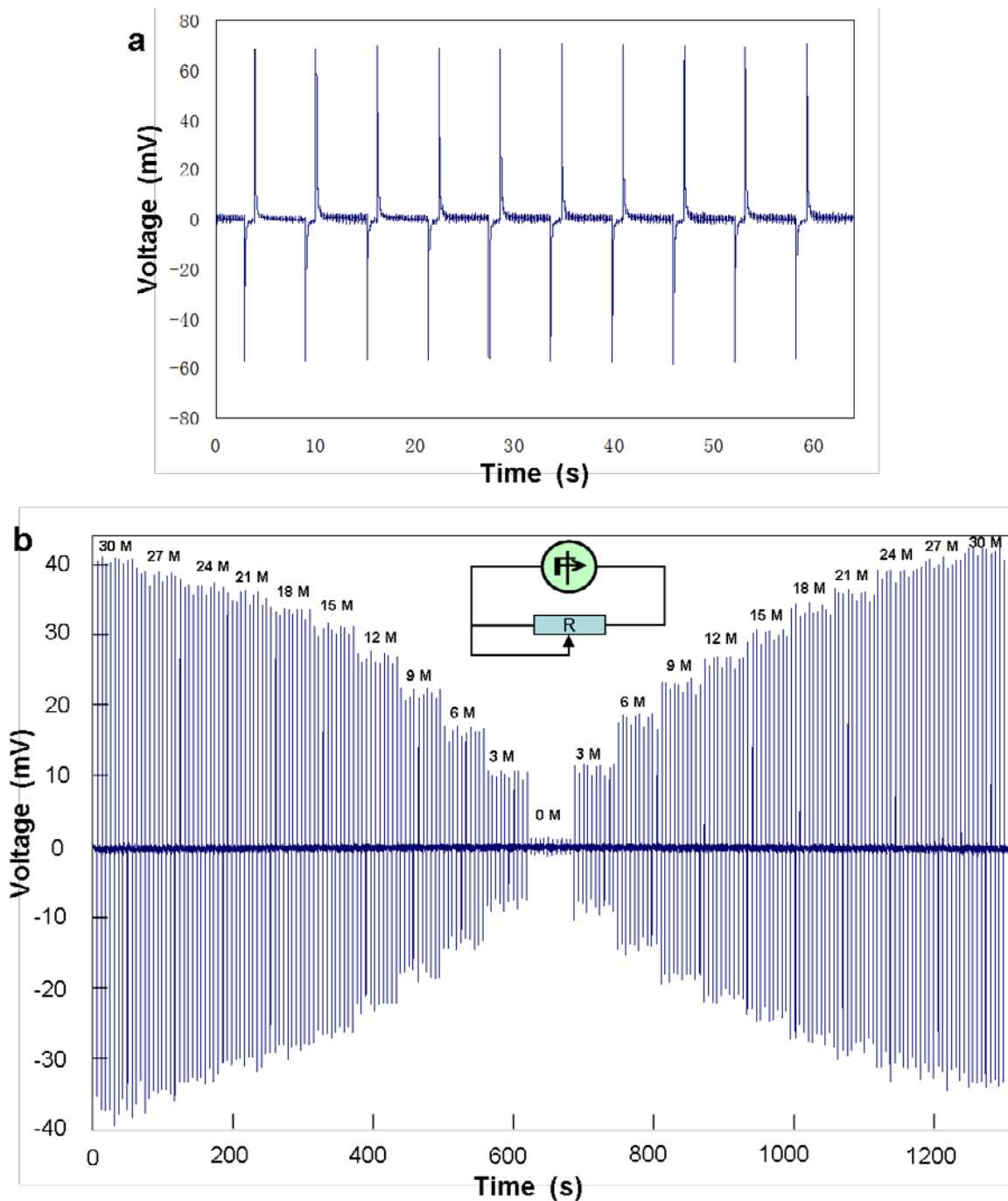
Figure S9 | (a) The open circuit voltage output of an VING. (b) When gradually changing the amount of loading resistance (from 0 to 30 MΩ), the magnitude of the voltage drop across the resistor changes accordingly. The voltage on the resistor is $V = V_0R/(R+r)$, where V_0 is the open circuit voltage of the VING, r is its inner resistance, and R is the resistance of the resistor.
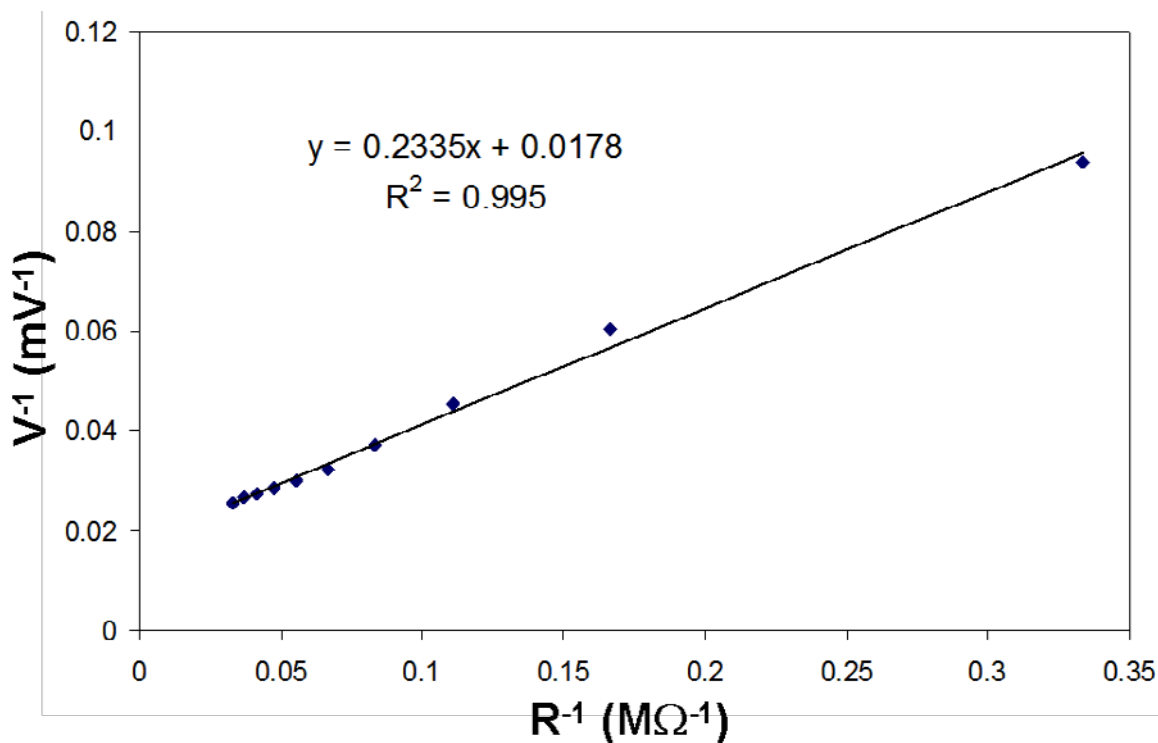
Figure S10 | Calculation of the VING's open circuit voltage and inner resistance using the data shown in Fig. S9.

$$\frac{1}{V} \quad \frac{r}{V_0} \quad \frac{1}{R} \quad \frac{1}{V_0}$$

$V_0 = 56$ mV

$r = 13$ MΩ

The linear fit of the data from Fig. S9 is exactly the result of linear circuit theory that uses the VING as a power source with a fixed output voltage of 56 mV.

What is the figure of merits for using ZnO nanowires?

In terms of the piezoelectric coefficient, ZnO may not be as favorable as other conventional piezoelectric materials. However, this is not the only merit that matters! Compared with other materials, like PZT and barium titanates, ZnO nanowires/nanobelts have several incompatible figures of merits, as stated in the following:

1. Extremely high elasticity that allows large degrees of bending without cracking as a result of nano-size[1-2], as shown in Fig. S11.

2. Resistance to fatigue even after 35 billion cycles of vibrations at the resonance frequency[3].

3. Large power density. The power density for ZnO was estimated to be 2.7 mW/cm^3, which is about ten times higher than that of PZT[4-5]. Studies have also shown that the piezoelectric coefficient of ZnO nanostructure is 14 times of its bulk[6].

4. Piezotronic effect. ZnO is a wide direct bandgap semiconductor that is ideal to build piezotronic nanodevices[7-12]. This unique application is unable to be accomplished using PZT or barium titanates.

5. Controlled growth on any type and shape substrates at low temperature (<100 C)[13-15], much lower than the temperature required to grow PZT. This figure of merit allows ZnO nanowires to grow at low temperature on any substrate and any shape substrate, exhibiting a huge advantage for scaling up at a low cost[16].

6. It is biocompatible, which have potential applications in *in-vivo* biosensors, and bio-diagnostics[17], while PZT may be bio-incompatible.

7. Environmental friendly. PZT and barium titanates have heavy metal ions and are not environmentally friendly.

By integrating all of the above facts, ZnO is a much better, much cheaper and environmentally friendly material for the applications we are proposing. One should not solely focus on the piezoelectric coefficient and takes it as the only figure of merit when we discuss about a material. Therefore, the use of ZnO nanowires for the applications we are proposing is likely the best solution.
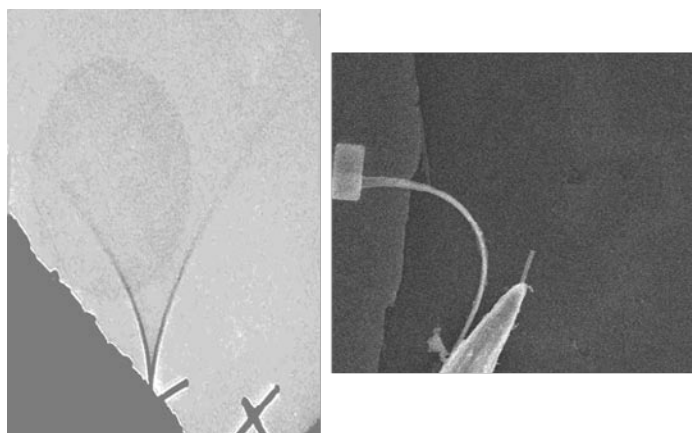

Figure S11. The ZnO nanowire is still elastic after more than 70° of bending.

References

1. Lucas, M., Mai, W. J., Yang, R. S., Wang, Z. L. & Riedo, E. Aspect ratio dependence of the elastic properties of ZnO nanobelts. *Nano Lett.* **7**, 1314-1317 (2007).

2. Song, J. H., Wang, X. D., Riedo, E. & Wang, Z. L. Elastic property of vertically aligned nanowires. *Nano Lett.* **5**, 1954-1958 (2005).

3. Gao, Z. Y., Ding, Y., Lin, S. S., Hao, Y. & Wang, Z. L. Dynamic fatigue studies of ZnO nanowires by in-situ transmission electron microscopy. *Phys. Status Solidi-Rapid Res. Lett.* **3**, 260-262 (2009).

4. Roundy, S., Wright, P. K. & Rabaey, J. A study of low level vibrations as a power source for wireless sensor nodes. *Comput. Commun.* **26**, 1131-1144 (2003).

5. Shen, D. N. *et al.* Micromachined PZT cantilever based on SOI structure for low frequency vibration energy harvesting. *Sens. Actuators A-Physical* **154**, 103-108 (2009).

6. Zhang, X. Q., Tang, Z. K., Kawasaki, M., Ohtomo, A. & Koinuma, H. Resonant exciton second-harmonic generation in self-assembled ZnO microcrystallite thin films. *J. Phys.-Condens. Matter* **15**, 5191-5196 (2003).

7. Wang, X. D. *et al.* Piezoelectric field effect transistor and nanoforce sensor based on a single ZnO nanowire. *Nano Lett.* **6**, 2768-2772 (2006).

8. He, J. H., Hsin, C. L., Liu, J., Chen, L. J. & Wang, Z. L. Piezoelectric gated diode of a single ZnO nanowire. *Adv. Mater.* **19**, 781-784 (2007).

9. Wang, Z. L. The new field of nanopiezotronics. *Mater. Today* **10**, 20-28 (2007).

10. Zhou, J. *et al.* Mechanical-electrical triggers and sensors using piezoelectric micowires/nanowires. *Nano Lett.* **8**, 2725-2730 (2008).

11. Zhou, J. *et al.* Flexible piezotronic strain sensor. *Nano Lett.* **8**, 3035-3040 (2008).

12. Hu, Y. F., Gao, Y. F., Singamaneni, S., Tsukruk, V. V. & Wang, Z. L. Converse Piezoelectric Effect Induced Transverse Deflection of a Free-Standing ZnO Microbelt. *Nano Lett.* **9**, 2661-2665 (2009).

13. Qin, Y., Wang, X. D. & Wang, Z. L. Microfibre-nanowire hybrid structure for energy scavenging. *Nature* **451**, 809-813 (2008).

14. Qin, Y., Yang, R. S. & Wang, Z. L. Growth of Horizonatal ZnO Nanowire Arrays on Any Substrate. *J. Phys. Chem. C* **112**, 18734-18736 (2008).

15. Xu, S., Lao, C., Weintraub, B. & Wang, Z. L. Density-controlled growth of aligned ZnO nanowire arrays by seedless chemical approach on smooth surfaces. *J. Mater. Res.* **23**, 2072-2077 (2008).

16. Greene, L. E. *et al.* Low-temperature wafer-scale production of ZnO nanowire arrays. *Angew. Chem. Int. Ed.* **42**, 3031-3034 (2003).

17. Li, Z. *et al.* Cellular Level Biocompatibility and Biosafety of ZnO Nanowires. *J. Phys. Chem. C* **112**, 20114-20117 (2008).